Journal Pre-proof

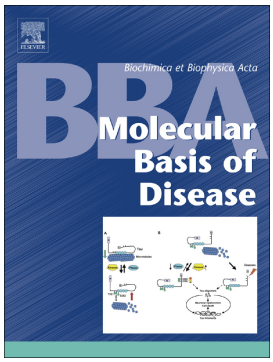

CAV1 unveils a novel therapeutic target for nephrolithiasis by modulating CaSR and ER stress

Yang Li, Baoyu Yang, Haozhen Wang, Wenqi Hu, Ting Liu, Xiuli Lu, Bing Gao

PII: S0925-4439(25)00096-1

DOI: https://doi.org/10.1016/j.bbadis.2025.167751

Reference: BBADIS 167751

To appear in: *BBA - Molecular Basis of Disease*

Received date: 11 November 2024

Revised date: 20 February 2025

Accepted date: 24 February 2025

Please cite this article as: Y. Li, B. Yang, H. Wang, et al., CAV1 unveils a novel therapeutic target for nephrolithiasis by modulating CaSR and ER stress, *BBA - Molecular Basis of Disease* (2025), https://doi.org/10.1016/j.bbadis.2025.167751

CAV1 unveils a novel therapeutic target for nephrolithiasis by modulating CaSR and ER stress

Yang Li[1,3,†], Baoyu Yang[2,†], Haozhen Wang[2], Wenqi Hu[1,3], Ting Liu[2], Xiuli Lu[2,*] Bing Gao[1,3*]

1. Department of Cell biology and Genetics, Shenyang Medical College, 146 Huanghe North Street, Shenyang 110034, China
2. Department of Biochemistry and Cell Biology, School of Life Science, Liaoning University, Shenyang 110036, China
3. Key Laboratory of Renal Calcification Disease Prevention and Treatment, 146 Huanghe North Street, Shenyang 110034, China

† Yang Li and Baoyu Yang contributed equally to this work and share first authorship.

* Address correspondence to Bing Gao, M.D. Ph.D. and Xiuli Lu, M.D.Ph.D

Bing Gao

Department of Cell Biology and Genetics, Shenyang Medical College, 146 Huanghe North Street, Shenyang 110034, China,

Tel.: +86-24-62215664

E-mail address: gaobingdr@hotmail.com

Xiuli Lu

The School of Life Science, Liaoning University, Chongshanzhong-Lu No.66, Huanggu-Qu, Shenyang 110036, China

E-mail address: luxiuli@lnu.edu.cn

Abstract

Nephrolithiasis is a complex disease resulted from abnormal crystal deposition in renal tissues. The crystal-cell interaction represents a critical step in kidney stone formation, involving numerous genes and proteins. We previously identified endoplasmic reticulum (ER) stress as a key biological process in the crystal-cell interactions, the precise mechanism of which has remained unclear. In the present study, we found that calcium oxalate monohydrate (COM) crystals induced an overload of intracellular Ca^{2+} and an upregulation of calcium-sensing receptor (CaSR) expression in the renal tubular epithelial cells HK-2, both of which were reversed by the CaSR inhibitor NPS2390 that also mitigated the COM-induced ER stress. The protein-protein interaction (PPI) network analysis of the genome-wide association studies (GWAS) data and the microarray data from kidney stone patients revealed that caveolin-1 (CAV1), epidermal growth factor receptor (EGFR), and the focal adhesion pathway formed a crucial intersection within the interactional networks. COM exposure induced HK-2 apoptosis, accompanied by a decrease in CAV1 protein levels and damage to EGFR-AKT signaling pathway, which was reversed by CAV1 overexpression. COM did not significantly affect CAV1 mRNA levels. Treatment with the proteasome inhibitor MG-132 prevented the downregulation of CAV1. CAV1 overexpression also inhibited ER stress and the upregulation of CaSR induced by COM. Similar results were observed in *in vivo* experiments. In conclusion, the present study suggests that CAV1 may be a promising target for nephrolithiasis therapy by modulating CaSR and ER stress.

Keywords: ER stress, PPI network, CaSR, CAV1, Kidney stone

1. Introduction

Nephrolithiasis, commonly known as kidney stones, is a complex multifactorial disease that results in abnormal crystal deposition in renal tissues. About 2–5% of the population in Asia and 8–15% in Europe and North America will develop kidney stones in their lifetime[1], with a recurrence rate of 50% over 10 years[2]. Calcium oxalate (CaOx) is the most common type of kidney stones, accounting for 70–80% of the total[2]. The interactions between nascent crystals and kidney cells constitute a critical step in the formation of kidney stones, involving numerous genes and proteins that form a complex interaction network[3-6]. We previously identified endoplasmic reticulum (ER) stress as a critical biological process in the crystal-cell interactions by analyzing the protein-protein interaction (PPI) networks derived from proteomic data related to kidney stones, which was confirmed both *in vitro* and *in vivo*[7]. However, the specific molecular mechanism by which CaOx crystals induce ER stress in renal tubular epithelial cells (RTECs) remains unclear.

ER serves as the primary storage site for intracellular calcium (Ca^{2+}), which is essential for maintaining cellular function and viability[8]. Disruptions in Ca^{2+} homeostasis can trigger ER stress and the unfolded-protein response (UPR) due to the accumulation of unfolded or misfolded proteins[9]. The calcium-sensing receptor (CaSR) is a G protein-coupled receptor located on the cell membrane that plays a key role in sensing extracellular Ca^{2+} and regulating Ca^{2+} balance[10, 11]. Activated CaSR can also facilitate the release of Ca^{2+} from ER via phospholipase C (PLC) / inositol-triphosphate (IP3)/diacylglycerol (DAG) pathway[12]. Studies on myocardial ischemia/reperfusion in rats have shown that activating CaSR with $GdCl_3$, a CaSR activator, induced ER stress and apoptosis while increasing the intracellular Ca^{2+} concentration and decreasing the ER Ca^{2+} concentration[13], suggesting that CaSR may participate in ER stress-induced apoptosis by affecting intracellular Ca^{2+} level. Furthermore, CaSR has been implicated in regulating the influx of extracellular Ca^{2+}[14, 15]. However, it remains to be clarified whether CaSR-mediated disruption of intracellular calcium homeostasis is involved in CaOx-induced ER stress in RTECs.

The occurrence of kidney stones is a complex process involving gene variation, changes in gene expression and disturbances in signal pathways. In order to identify important genes and pathways that relate to kidney stone formation, the combined analysis based on genome-wide association studies (GWAS) and microarray data associated with calcium stones would be valuable to be performed. We therefore enriched and overlapped these data and found that the gene *CAV1* and the focal adhesion pathway may play a critical role in crystal-cell interaction. Caveolin-1 (CAV1) encoded by *CAV1* is a major structural protein in caveolae that is a central node for plasma membrane signaling in cell growth and Ca^{2+} regulation[16, 17]. Evidence indicates the co-localization of CAV1 and CaSR at the plasma membrane in the human cell line Saos-2 and the human umbilical vein endothelial cells (HUVECs), with conflicting effects of CAV1 on CaSR-mediated extracellular Ca^{2+} influx[14, 15]. During the process of kidney stone formation, whether CAV1 regulates CaSR-mediated intracellular Ca^{2+} homeostasis and participates in ER stress remains to be clarified. In addition, the epidermal growth factor receptor (EGFR), a member of the receptor tyrosine kinase (RTK) family, interacts with CAV1 in the focal adhesion pathway to promote cell survival and anti-apoptosis. CaSR, CAV1 and EGFR are all located in the caveolae of cell membranes, suggesting their significant roles in the key biological processes during crystal-cell interaction.

In the present study, we explored the detailed mechanisms of CaOx-induced ER stress, finding that CaSR-mediated upregulation of intracellular Ca^{2+} concentration leads to ER stress, subsequently decreasing the expression of CAV1 through post-translational degradation. CAV1 degradation may exacerbate ER stress through a negative feedback loop, impacting cell survival together with the EGFR/AKT signaling pathway. These findings shed light on the mechanism of ER stress in nephrolithiasis and may potentially unveil a novel and crucial target for nephrolithiasis therapy.

2. Materials and Methods

2.1 GWAS Data Set

Susceptibility SNPs associated with kidney stones were identified from four GWAS datasets. 22 SNPs were derived from the study of Rungroj *et al*. who genotyped 101 patients and 105 controls in Thailand[3]. The top 100 susceptibility SNPs were taken from the study of Urabe *et al*., who undertook a three-stage GWAS using 5,892 Japanese nephrolithiasis cases and 17,809 controls[6]. 34 SNPs were selected from Thorleifsson *et al*.'s GWAS study of 3,773 cases and 42,510 controls from Iceland and the Netherland[5], while 105 SNPs were obtained from Oddsson *et al*.'s GWAS study of 5,419 kidney stone cases and 279,870 controls from Iceland[4]. Taking a 500 kb window centered on a given SNP, we extracted SNPs with $r^2 > 0.8$ to the given SNP, using the 1000 Genomes Pilot 1. These SNPs were mapped onto seed genes using SNP Annotation and Proxy Search (SNAP), which identified SNPs using physical distance and linkage disequilibrium[18].

2.2 Microarray Data Set

A gene expression profile from Randall's Plaque (RP) tissue was obtained from the GEO database (GSE73680) as reported by Taguchi *et al*.[19]. The study conducted a microarray analysis of 62 samples, comparing gene expressions of the Randall's Plaque tissues (P group) and the normal papillary tissues (N group) of calcium stone formers, and the normal papillary tissues of patients without any kidney stones (C group). A total of 50,739 genes were analyzed in the study. The microarray data from the N group and C group were processed using GEO2R (https://www.ncbi.nlm.nih.gov/geo/geo2r).

2.3 PPI Network Construction and assessment

Different candidate genes and proteins were integrated into a reliable protein-protein interaction database using InWeb[20]. Permutation tests were used to identify genes and proteins significantly linked by PPI networks. Highly connected genes and proteins were identified using the GeneNet Toolbox[21]. PPI networks were visualized using Cytoscape[22]. The "Network Analyzer" Cytoscape plug-in was utilized to

analyze networks based on topological parameters like node degree and Betweenness Centrality (BC). Node degree refers to the number of edges linked to a particular node, while BC quantified the relative importance of an edge or node by considering the number of shortest paths that pass through it. Nodes with high node degree and high BC, or genes located at the periphery of a network but with high Edge Betweenness, were considered to be hub genes, potentially serving important biological functions. Backbone genes that were considered to be among the top 10% of hub genes, were determined by their ranking in terms of Node degree, BC, and Edge Betweenness.

2.4 Gene Ontology and KEGG Pathway Analysis

Genes identified above were analyzed for Gene Ontology (GO) and KEGG pathway enrichments using DAVID (http://david.abcc.ncifcrf.gov/)[23]. GO terms examined biological processes (BP), cellular components (CC), and molecular functions (MF). A threshold comprising a *p*-value < 0.05 and a false discovery rate (FDR) < 0.1 was considered statistically significant. Cumulative changes in functional categories were identified by overlap, using Venn diagrams (http://bioinformatics.psb.ugent.be/webtools/Venn/).

2.5 Study Participants

A total of 318 unrelated patients with kidney stones from Northeastern China were included in the present study. The control group consisted of 1,170 normal participants from the East Asian population, as documented in the 1000 Genomes Project database. All patients in this study were Chinese Han people. The study was approved by the Shenyang Medical College Institutional Review Board and informed consent was obtained from all participants. Genomic DNA was extracted from peripheral blood by using the RelaxGene Blood DNA System (Tiangen, China).

2.6 High-Resolution Melting (HRM) Analysis

HRM analysis was conducted as previously described[24]. Briefly, genotyping for SNP rs6867 (G>A) in the *CAV1* gene was performed in a 96-well plate using the HRM analysis kit (Tiangen, China). The forward primer for the human *CAV1* gene was 5'-CCCTGCTCAGTAAAGCACTTGC-3', while the reverse primer was 5'-

CAAAGGGATGCTTGGATTAGGT-3'. Samples identified as GG and GA through Sanger sequencing were selected as positive controls. For each experiment, normalization settings and reference genotypes remained consistent, and each sample was tested independently at least three times.

2.7 Cell culture

HK-2 cells were obtained from the Cell Resource Center of Life Sciences, Chinese Academy of Sciences (Shanghai, China). Cell culture was undertaken using Dulbecco's modified Eagle's medium (DMEM) containing 4.5 g/L glucose, supplemented with 10% (v/v) fetal bovine serum, 1% penicillin-streptomycin, and 0.45 mM L-glutamine. Cells were equilibrated at 37°C using 5% CO_2 and 95% O_2.

2.8 Measurement of intracellular Ca^{2+} level

The intracellular Ca^{2+} level was measured with a calcium ion fluorescent probe Fluo-4 AM. Briefly, HK-2 cells seeded on glass coverslips were incubated with Fluo-4 AM (4 μM in PBS) at 37℃ for 1 hour. After fixation with 4% paraformaldehyde, the nucleus was stained with the antifade mounting medium with DAPI (Beyotime, China). The resultant fluorescence was captured by fluorescence microscopy (Olympus, Japan). The fluorescent intensity was determined by ImageJ software.

2.9 TUNEL assays

HK-2 cells were exposed to 100 μg/mL calcium oxalate monohydrate (COM) for 24 or 48 hours before *in situ* apoptosis assays were undertaken. Apoptosis was analyzed using the TUNEL method. An *in situ* apoptosis kit (Vazyme, Nanjing, China) was used, following manufacturer's instructions. Cells were also incubated with the antifade mounting medium with DAPI (Beyotime, China), and then observed using a fluorescence microscope (Olympus, Japan). The apoptosis rate was calculated as the percentage of apoptotic cells to adherent cells.

2.10 Quantification of mRNA

Total RNA was extracted using TriZol (Invitrogen). Reverse transcription was undertaken using 500 ng of total RNA, making use of PrimeScript^{TM} RT Master Mix reverse transcription kit (Takara RR036A). Real-time PCR amplification of reverse-

transcribed RNA was undertaken using TB Green™ Premix Ex Taq™ (Takara RR820A), with a 20 μl system. Results were expressed as $2^{-\Delta Ct}$ values, with $\Delta CT = Ct_{CAV1} - Ct_{GAPDH}$. Primers are as follows:

Human *CAV1* forward: TGGTCAACCGCGACCCTAA,

Human *CAV1*reverse: TCGTCACAGTGAAGGTGGTGAAG;

Human *GAPDH* forward: GGCACAGTCAAGGCTGAGAATG,

Human *GAPDH* reverse: ATGGTGGTGAAGACGCCAGTA.

Rat *Cav1* forward: CGGGAACAGGGCAACATCTAC,

Rat *Cav1* reverse: CTTCTGGTTCCGCAATCACATC;

Rat *Gapdh* forward: TGCTGAGTATGTCGTGGAGTCTA

Rat *Gapdh* reverse: AGTGGGAGTTGCTGTTGAAATC

2.11 Western blotting analysis

Protein preparation and western blotting analysis were undertaken as described previously[25]. Briefly, cell lysates were separated by SDS-PAGE and transferred to polyvinylidene difluoride membrane (Immobilon®-P, Merck Millipore, Co, USA). Rabbit anti-XBP1 antibody (bs-1668R), anti-GRP78/Bip antibody (bs-1219R) and anti-ATF6 antibody (bs-1634R) were purchased from Bioss (Beijing, China). Rabbit GADD153/CHOP (E1A0629) was purchased from EnoGene (Nanjing, China). Phospho-EGF receptor (Tyr1068) rabbit mAb (#3777), phospho-AKT (Ser473) rabbit mAb (#4060), EGF receptor (D38B1) rabbit mAb (#4267), AKT antibody (#9272), and cleaved caspase-3 (Asp175) antibody (#9661) were purchased from Cell Signaling Technology (Beverly, MA). Rabbit CaSR polyclonal antibody (19125-1-AP) and Rabbit phospho-PERK polyclonal antibody (29546-1-AP) were purchased from Proteintech (Wuhan, Hubei, China). Anti-caveolin-1 mouse monoclonal antibody (EM40728) was obtained from HuaBio (Hangzhou, Zhejiang, China). Blots were probed for primary antibodies, followed by incubation with horseradish peroxidase-conjugated anti-rabbit IgG antibody. Proteins were visualized using enhanced chemiluminescence (ECL) reagents (MeilunBio, Dalian, Liaoning, China). Images of blotted membranes were acquired using a LAS-1000 lumino-image analyzer (Fujifilm,

Tokyo, Japan). Densitometry analysis was undertaken using the software ImageJ (http://imagej.net/ImageJ).

2.12 Immunocytochemical analysis

To investigate the effect of COM exposure on CAV1 expression, HK-2 cells were incubated with anti-caveolin-1 mouse monoclonal antibody for 60 minutes after fixation and blocking, followed by ABflo488-conjugated goat anti-mouse IgG (ABclonal, AS037). Images were acquired using a fluorescence microscope (Olympus, Japan). ImageJ software was used to determine the fluorescent intensity.

2.13 Adenovirus transfection

The recombinant adenovirus encoding the whole coding sequence of human *CAV1* (NM_001753.5) was obtained from HanBio Co. Ltd (Shanghai, China) and was termed as HBAD-Adeasy-h-CAV1-3xflag-Null (HBAD-hCAV1). HBAD-Null served as a negative control adenovirus. HK-2 cells were cultured using DMEM growth medium in 60 mm cell culture dishes at a starting density of 3×10^5 cells per dish. HK-2 cells were grown to 50% confluence, and transfected with HBAD-hCAV1 at 20 multiplicity of infection (MOI) for 48 hours, which followed by exposure to COM.

2.14 Atomic Absorption Assay

Atomic absorption was used to determine the crystal adhesion on the cell surface. In this experiment, CAV1 overexpressing recombinant adenovirus labeled with GFP (pHBAd-hCAV1) and the control adenovirus pHBAd-GFP previously synthesized was transfected into HK-2 cells for 48 hours. COM were then suspended in DMEM at a concentration of 2 mg/mL and treated with ultrasound for 15 minutes. Cells were exposed to 100 μg/mL COM for five minutes. Non-adherent crystals were removed by washing the 6-well plate with PBS solution three times. COM that had adhered to cells were collected with 2 mL of 6 M HCl. Quantitative analysis of the adherent crystals was undertaken by measuring the calcium concentration using atomic absorption.

2.15 Animal Models

Eight-week-old male Sprague-Dawley (SD) rats were divided into treatment (n = 25) and control (n = 5) groups and monitored at intervals of 0, 2, 4, 6, and 8 weeks. The

treatment group received 0.75% ethylene glycol (EG) via drinking water. The control group was given natural water. All animal experiments were reviewed and approved by the Animal Committee of Shenyang Medical College.

2.16 Immunohistochemical staining

Formalin-fixed and paraffin-embedded (Servicebio Technology, Wuhan, China) tissue of multiple groups were incubated with anti-CAV1 (Abclonal, Wuhan, China) (1 μg/mL). After washing with PBS, slides were reacted with anti-rabbit HRP IgG1 (Servicebio technology, Wuhan, China). Protein expression was determined based on the extent and intensity of staining, as observed for each slide.

2.17 Statistical Analysis.

For the PPI networks, a permutation test was performed to evaluate network reliability, using the GeneNet Toolbox. For the GO and KEGG analysis, a p value < 0.05 and an FDR < 0.1 were considered statistically significant. For other experiments, statistical analysis was performed by utilizing the GraphPad Prism version 7.0 software. Each experiment was replicated at least three times independently and the values were expressed as the mean ± SD or SEM. Comparisons were analyzed with the one-way or two-way ANOVA test. A p value < 0.05 was considered statistically significant.

3 Results

3.1 CaSR-mediated intracellular Ca^{2+} overload participated in the COM-induced ER stress in HK-2 cells.

Our previous study has demonstrated that exposure to COM led to ER stress in HK-2 cells [7], but the underlying cause remained unclear. ER is the main intracellular Ca^{2+} storage. Disturbance of intracellular Ca^{2+} homeostasis that is closely related to CaSR could result in ER stress[12, 13]. To investigate whether COM-induced ER stress in HK-2 cells was related to CaSR-mediated perturbations in intracellular Ca^{2+} homeostasis, we measured the intracellular Ca^{2+} level with Fluo-4 AM, a widely used fluorescent probe of Ca^{2+}. The HK-2 cells exhibited significantly increased green fluorescence 6 hours after COM exposure, indicating an overload of intracellular Ca^{2+}

induced by COM (Figure 1a and b). Notably, pretreatment with the CaSR inhibitor NPS2390 significantly attenuated the COM-induced upregulation of intracellular Ca^{2+} level, suggesting the involvement of CaSR in the disturbance of intracellular Ca^{2+}. Furthermore, the expression levels of CaSR and ER stress-specific markers, including glucose-regulated protein 78/binding immunoglobulin protein (GRP78/Bip) and C/EBP homologous protein (CHOP), were evaluated under the same conditions. A marked increase in the expression of these three proteins was observed following COM exposure, which was reversed by NPS2390 (Figure 1c-f). Upon ER stress, three signaling pathways of the unfolded protein response (UPR) that are characterized respectively by the activation of ATF6, IRE1-XBP1, and PERK-eIF2α are activated to deal with the accumulation of unfolded or misfolded proteins in ER [26]. NPS2390 also inhibited the increase of ATF6, XBP-1 expression and the phosphorylation level of PERK induced by COM (Figure 1c and g-i). Taken together, these results suggest that CaSR-mediated intracellular Ca^{2+} overload is intricately linked to COM-induced ER stress in HK-2 cells.

3.2 The integrated analysis of genetic variants and differentially expressed gene networks revealed that CAV1 may play a key role in the development of kidney stones

The pathogenesis of kidney stones is a multifaceted process involving numerous genes and proteins, forming a complex interaction network. Network analysis is a tool to delve into the intricate networks linking genes and proteins to the molecular mechanisms underlying the disease etiology[18]. A workflow corresponding to our network analysis is shown in Figure 2a. Firstly, susceptibility SNPs associated with kidney stones were selected from four GWAS datasets and 261 candidate SNPs that mapped to 199 susceptibility genes were obtained after removing duplicates (Supplementary Table 1). These genes were translated into protein sequences to construct a PPI network and assessed using a permutation test (n = 1000 permutations). We found a direct network comprising 38 proteins (Figure 2b). The interconnectivity indicated a significantly greater number of edges than would be expected by chance (*p*

= 0.019). This suggests that these 38 genes may increase the risk of kidney stones by perturbing molecular networks involved in nephrolithiasis. The top 10% of nodes were designated as hub genes including *EGFR*, *AR*, *CAV1*, and *CDH1* (Table 1). KEGG pathway analysis revealed enrichment in pathways like the Rap1 signaling pathway, focal adhesion, and pathways in cancer (Figure 2c). This comprehensive workflow and network analysis provides insights into the genetic factors contributing to kidney stone formation.

To further investigate kidney stone-related genes with expression change, a gene expression profile (GSE73680) of kidney stone patients was obtained from the GEO database. In the comparison of the C group and N group, 2,156 genes were upregulated and 267 genes were downregulated with log2 fold change (|log2FC| > 2). A PPI network was also constructed, revealing 345 proteins in the direct network (Figure 2d). The permutation test indicated that there were more edges than would be expected by chance (p = 0.0009). Moreover, this network was enriched in several KEGG pathways, including the PI3K-AKT signaling pathway, neuroactive ligand-receptor interaction, pathways in cancer, and focal adhesion (Figure 2e).

To clarify the most consistent pathogenic factors underlying kidney stones, our analysis focused on examining the intersection of the genetic variant network and differentially expressed network. Six genes (*DMBT1*, *ZNF408*, *CAV1*, *LRP2*, *CAV2*, and *HSPG2*) and two signaling pathways (focal adhesion and proteoglycans in cancer) formed the intersection between the two networks (Figure 2f and g). CAV1 and EGFR are known to be critical members of the focal adhesion signaling pathway, which is important in cell proliferation, gene expression, and cell survival. Furthermore, the SNP rs6867 variant of the *CAV1* gene has been reported to be associated with the risk of kidney stones in the northeastern Thai population[3]. To investigate this association further, we conducted a genotyping experiment on SNP rs6867 in kidney stone patients from Northeastern China (Figure 2h-j), and utilized the genotypes of the East Asian population from the 1000 Genomes Project database as controls. The statistical analysis results (Table 2) showed that carriers with the GA genotype were more prevalent among

patients compared to the controls (p = 0.0451, 95% CI 1.001 - 4.181). Similarly, the frequency of the A-allele in cases was higher than that in the controls (p = 0.0464, 95% CI 0.997 - 4.117), suggesting an increased risk of kidney stones.

Taken together, these findings suggest that CAV1 may play a crucial role in the development of kidney stones. Consequently, we directed our focus towards CAV1 and its influence on crystal-cell adhesion.

3.3 COM-induced post-translational degradation of CAV1 impaired the EGFR/AKT cell survival signaling pathway

CAV1, as a key component of caveolae, plays a crucial role in plasma membrane signaling related to cell growth and can influence cell survival via the EGFR/AKT pathway[27]. Here, we investigated the impact of COM on CAV1 expression and the EGFR/AKT signaling pathway in HK-2 cells. Apoptosis was assessed in HK-2 cells following exposure to 100 μg/mL COM for 24 and 48 hours using TUNEL and DAPI assays (Figure 3a and b). The number of positive-apoptotic cells in the COM-treated group was significantly higher than that in the control group. Severe damage to caveolae was observed using immunocytochemical analysis when compared to the control group (Figure 3c and d). Western blotting analysis showed a noticeable decrease in CAV1 protein expression and EGFR/AKT phosphorylation levels 24 hours after COM exposure (Figure 3e-h). These findings demonstrated that impaired CAV1-EGFR/AKT signaling pathway might be associated with COM-induced HK-2 apoptosis.

Subsequently, we investigated the reasons for the decline in CAV1 protein levels induced by COM. RT-PCR analysis of CAV1 mRNA levels revealed no significant changes after COM exposure (Figure 3i), indicating that a post-transcriptional mechanism was involved in the reduction of CAV1 protein. Post-translational degradation, which is closely related to ER stress, is a common mechanism for post-translational regulation. We employed the proteasome inhibitor MG132 to block the post-translational degradation, analyzing the concomitant changes in CAV1 expression. As shown in Figure 3j, compared to the control group, there was a marked reduction in

CAV1 expression levels in cells treated with COM alone, while simultaneous treatment with MG132 and COM resulted in a significantly higher level of CAV1 than that in the cells treated with COM alone, demonstrating the ability of MG132 to inhibit the proteasomal degradation of CAV1. These findings suggest that COM induces the post-translational degradation of CAV1.

ER stress is an adaptive response initiated by cells in response to ER dysfunction or the misfolded proteins in the ER, subsequently activating the UPR and proteasome degradation to restore ER protein homeostasis[28]. Our results suggest that COM-induced ER stress through the activation of CaSR, adversely affects the CAV1-EGFR/AKT signaling pathway potentially by initiating the post-translational degradation of CAV1, ultimately resulting in cell apoptosis.

3.4 CAV1 overexpression inhibited HK-2 apoptosis and reduced crystal-cell adhesion.

To further investigate the role of CAV1 in COM-induced HK-2 apoptosis, we constructed the recombinant adenovirus HBAD-hCAV1 to overexpress CAV1 and used HBAD-Null as a negative control. Western blotting confirmed successful overexpression of CAV1 driven by recombinant adenovirus (Figure 4a and b). TUNEL analysis revealed a significant decrease in TUNEL-positive cells after COM exposure in the HBAD-hCAV1 group compared to the HBAD-Null group (Figure 4c-d). Additionally, CAV1 overexpression notably inhibited COM-induced activation of caspase 3 (cleaved caspase 3) (Figure 4e-f), indicating its role in preventing apoptosis. Crystal-cell adhesion is a crucial step in the formation of kidney stones. By detecting the Ca^{2+} concentration on the cell surface with atomic absorption, we found a significant decrease in the CAV1 overexpression group compared to the control group (Figure 4g), suggesting that CAV1 overexpression could impede COM crystal adhesion to cell surfaces, thereby safeguarding HK-2 cells from COM-induced damage. Further western blotting analysis exhibited that CAV1 overexpression effectively inhibited the COM-induced decrease in phosphorylated EGFR and the AKT (Figure 4h-j), implying that restoring CAV1 expression can block cell-crystal interaction and protect HK-2 cells

by repairing the EGFR-AKT survival signaling pathway.

3.5 CAV1 overexpression inhibited COM-induced ER stress

Previous researches have shown that CAV1 could regulate CaSR-mediated Ca^{2+} homeostasis imbalances in HUVECs and Saos-2cells [14, 15]. However, the effect of CAV1 on COM-induced intracellular Ca^{2+} increase remains unclear. In the present study, we observed CAV1 overexpression inhibited the increase of the intracellular Ca^{2+} level 6 hours after COM exposure, as measured by Fluo-4 AM (Figure 5a and b). Western blotting analysis revealed that compared to the HBAD-Null group, CAV1 overexpression suppressed the upregulation of ER stress markers Bip, CHOP, XBP-1 and the phosphorylated PERK from 6 hours to 24 hours, but did not affect the expression of ATF6 (Figure 5c-h). Additionally, the expression of CaSR induced by COM was also lower in CAV1-overexpressing cells than that in the HBAD-Null group, suggesting that CAV1 overexpression inhibited the CaSR expression (Figure 5c and i). These results indicate that COM-induced CAV1 degradation possibly exacerbates CaSR-mediated ER stress, while CAV1 overexpression might alleviate ER stress by regulating CaSR-mediated Ca^{2+} homeostasis disorder.

3.6 CaSR-CAV1-EGFR/AKT signaling axis was altered in rat renal crystal models and kidney stone patients

To provide additional *in vivo* evidence, SD rats were treated with 0.75% EG for 2, 4, 6, and 8 weeks. Renal crystals were observed from week 2 to week 8 (Figure 6a). Clear inflammation was seen at week 8, especially in the renal cortex (Figure 6b), coinciding with a significant decrease in CAV1 expression (Figure 6c and d). This is consistent with the well-known role of CAV1 as an inflammatory inhibitor[29]. The immunohistochemistry experiments also showed that the expression of CAV1 in the renal medulla was obviously reduced from week 2 to week 6 while that in the renal papilla was reduced remarkably at week 6 and week 8 (Figure 6c-f). Western blotting analysis displayed a pronounced downregulation of the CAV1 protein in the rat kidney from week 6 after EG treatment (Figure 6g and h), but the mRNA level of CAV1 displayed no significant changes (Figure 6i). Moreover, the expression of CaSR

demonstrated a remarkable increase from week 2 after EG treatment, while the phosphorylation levels of EGFR and AKT showed a marked decrease following EG treatment (Figure 7a-d). Our previous experiments found that ER stress occurred in the kidneys of EG-treated SD rats[7]. Collectively, these findings suggest that crystal-induced CAV1 reduction *in vivo* may be linked to CaSR-mediated ER stress.

To investigate the alterations in the CaSR-CAV1-EGFR/AKT signaling axis in kidney stone patients, we extracted gene expression data from GSE73680 in GEO datasets. Compared to the control (C group), both the normal papillary tissue (N group) and Randall's plaque tissue (P group) from patients with calcium stones exhibited elevated CaSR expression levels, although this increase was not statistically significant (Supplementary Figure 1a), which may be influenced by various factors, including tissue samples, detection methods, and statistical analysis. In contrast, there was a significant decrease in CAV1 expression levels (Supplementary Figure 1b). Additionally, the expression levels of EGFR and AKT1/AKT2/AKT3 showed varying degrees of reduction in both the N and P groups compared to the C group (Supplementary Figure 1c-f). These results suggest that the CaSR-CAV1-EGFR/AKT signaling axis is also compromised in kidney stone patients, which is consistent with the results observed at the cellular and animal levels.

In summary, these *in vivo* results align with the *in vitro* findings, supporting the conclusion that the CaSR-CAV1-EGFR/AKT signaling axis plays an important role during the formation of kidney stones.

4 Discussion

ER stress is an important biological process in the formation of kidney stones. In the current study, we delved into the mechanism and the subsequent influence of ER stress induced by COM, discovering that COM triggered an increase in intracellular Ca^{2+} level by upregulating CaSR expression, leading to ER stress. To relieve ER stress, HK-2 cells initiated the post-translational degradation of proteins. However, sustained ER stress destroyed the structure of caveolae through CAV1 degradation and impaired

the EGFR-AKT cell survival signaling pathway, ultimately causing HK-2 apoptosis. On the contrary, CAV1 overexpression restored the EGFR-AKT signaling pathway and inhibited the CaSR-mediated ER stress, thereby protecting HK-2 cells from COM-induced apoptosis (Figure 8). These results may provide novel therapeutic targets for the treatment of nephrolithiasis.

Ca^{2+} is an important mediator for maintaining cellular homeostasis and is strictly regulated by various hormones and signaling molecules including CaSR. CaSR, a G-protein coupled receptor present as a dimer in the plasma membrane, is essential for renal calcium regulation. Mutations in CaSR have been linked to hypercalciuria and calcium nephrolithiasis, making it a potential candidate gene for calcium stone formation [30, 31]. Activation of CaSR by extracellular Ca^{2+} triggers a cascade of events, including the activation of PLC by the Gq protein. PLC decomposes phosphatidylinositol 4,5-diphosphate (PIP2) into DAG and IP3, leading to the activation of receptor-operated Ca^{2+} entry (ROCE) and store-operated Ca^{2+} entry (SOCE), promoting a Ca^{2+} influx[32]. Prolonged Ca^{2+} influx can disturb the intracellular Ca^{2+} level, triggering some harmful reactions such as oxidative stress and ER stress[33]. SOCE is an ER-dependent Ca^{2+} entry mechanism that is stimulated by the depletion of ER Ca^{2+}[34]. Gombedza *et al.* found that SOCE-mediated Ca^{2+} influx was the main mechanism of crystal-induced ER stress in human proximal tubular cells[33]. CaSR is an upstream signaling molecule of SOCE, and we discovered that COM exposure increased the expression of CaSR and intracellular Ca^{2+} level in HK-2 cells. Treatment with CaSR inhibitor NPS2390 effectively reduced intracellular Ca^{2+} level, thus alleviating COM-induced ER stress. In addition, Li *et al* observed that NPS2390 decreased crystal adhesion and renal hypofunction in rats treated with 1% EG[35]. These results demonstrate the important role of CaSR in the formation of kidney stones and provide insights into the mechanism of crystal-induced ER stress, highlighting the role of CaSR-mediated Ca^{2+} influx.

With the development of high throughput detection technology, omics research has emerged as an important approach to study the pathogenesis of diseases. Despite

the increased efficiency of genomic, transcriptomic, and other large-scale kidney stone studies compared to traditional approaches, they still have many limitations. For examples, while GWAS can identify susceptibility variants at the DNA level, its utility is hindered due to a paucity of information concerning gene and protein expression. Moreover, different sample sizes, racial variation, and geographical and environmental stratification also affect the veracity of GWAS[36]. Altered gene expression identified by microarray analysis seldom correlates monotonically with corresponding protein expression and often contains much noise and minor secondary signals. To address these challenges, we integrated two studies at different levels to obviate limitations and pinpoint the key pathogenic factors underlying the formation of kidney stones. Firstly, we integrated the top-ranked susceptibility SNPs from four GWAS datasets conducted on diverse populations, including Japan, Iceland, the Netherlands, and Thailand, providing a comprehensive view of genetic variation linked to nephrolithiasis. Secondly, we constructed a direct interaction network and assessed its statistical robustness using a permutation test, generating authentic interaction networks at different levels. Subsequently, we extracted core networks from each direct network to highlight essential protein components implicated in the kidney stone formation. Finally, we identified common genes and pathways by comparing distinct networks, which are more likely to play a significant role in the risk of kidney stone formation. These rigorous strategies aim to ensure the accuracy and reliability of our findings.

Through the integrated analysis of omics, we identified that CAV1 and the focal adhesion pathway may play a crucial role in kidney stone formation, a process that is complex and closely related to RTECs injury, which is considered the driving factor of crystal precipitation and cellular adhesion[37]. Caveolae, functional invaginations of the plasma membrane, rely on CAV1 as their primary structural and functional protein. Limited studies have explored the impact of CAV1 on kidney stone formation, but Cao *et al*. demonstrated that disrupting the *CAV1* gene could impair renal calcium reabsorption, leading to hypercalciuria[38]. In the present research, we found that exposure of HK-2 cells to COM induced apoptosis, accompanied by the destruction of

the caveolae structure and a significant decrease in CAV1 protein levels. Similarly, experiments i*n vivo* showed that the formation of renal crystals and the appearance of kidney inflammation were also accompanied by an obvious decrease in CAV1 expression. EGFR is a member of the RTK protein family in the focal adhesion pathway. There is compelling evidence that CAV1 and EGFR are involved in cell survival and anti-apoptosis[39], and that CAV1 has a crucial role in EGFR-induced cell proliferation and migration[40, 41]. In *CAV1*-silenced HLE cells, the transactivation of EGFR and activation of the PI3K/AKT pathway are attenuated[42]. Here, we discovered that the phosphorylation levels of EGFR and AKT decreased significantly with the COM-induced RTECs apoptosis and crystals formation in rat renal. However, CAV1 overexpression effectively mitigated COM-induced apoptosis, reduced crystal adhesion to HK-2 surfaces, and inhibited the decline in EGFR and AKT phosphorylation levels, indicating the involvement of the CAV1-EGFR/AKT signaling axis in COM-induced RTECs injury. Recently, Yang *et al*. discovered that CAV1 could ameliorate autophagy-dependent ferroptosis through the LRP6/Wnt/β-Catenin axis and finally alleviate CaOx stone formation[43], further demonstrating the protective function of CAV1 on renal cells.

In the present study, we observed a non-statistically significant change in *CAV1* mRNA levels following crystal deposition, while the proteasome inhibitor MG132 significantly mitigated the COM-induced decrease in CAV1 protein levels, suggesting that the post-translational degradation participated in the reduction in CAV1 protein. CAV1, a membrane protein, has both its N-terminus and C-terminus situated in the cytoplasm. The N-terminus comprises six lysine residues (Lys5/26/30/39/47/57), which are potential sites for ubiquitination[44]. Previous studies have reported the ubiquitination and degradation of CAV1 under pathological conditions. For instance, Lee *et al*. demonstrated that the E3 ubiquitin ligase ZNRF1 promotes the ubiquitination and degradation of CAV1, leading to enhanced production of pro-inflammatory cytokines and inhibition of anti-inflammatory cytokines[45]. Hayer *et al*. identified that CAV1 was ubiquitinated and directed to intralumenal vesicles in endolysosomes for

degradation[46]. However, whether COM-induced CAV1 protein decline is related to the ubiquitin-proteasome degradation remains to be further investigated.

As mentioned above, caveolae are functional invaginations that contain multiple proteins, such as agonist receptors and ion channels that are crucial for intracellular Ca^{2+} signaling[47]. Evidences support the co-localization of CAV1 and CaSR at the plasma membrane[14, 15, 48], but the regulatory effect of CAV1 on CaSR-mediated Ca^{2+} entry seems different across cell types. In cultured human Saos-2 cells, the introduction of CAV-1 antisense oligodeoxynucleotide attenuated Ca^{2+} entry, suggesting an upregulation of CaSR function mediated by CAV1[14]. In human umbilical vein endothelial cells, an acute caveolae disruption with filipin or transfection with siRNA targeted to CAV-1 augmented the Spermine (a CaSR agonist)-induced increase in intracellular Ca^{2+} concentration, indicating that CAV1 inhibits the CaSR-induced extracellular Ca^{2+} influx[15]. In addition, CAV1 inhibits Pneumolysin-induced Ca^{2+} influx in endothelial cells by protecting the integrity of cell membranes[49]. In HK-2 cells, we demonstrated CAV1 overexpression reduced the intracellular Ca^{2+} levels and alleviated ER stress induced by COM, potentially through modulation of CaSR function. Specifically, the caveolin scaffolding domain at the N-terminus of CAV1 could directly interact with the G protein α subunits, which are essential mediators in the CaSR-activated PLC/IP3/DAG signaling pathway. The observed downregulation of the CaSR-mediated increase in intracellular Ca^{2+} levels by CAV1 may be attributed to the inhibition of the Gα subunit by CAV1[15]. Furthermore, CAV1 may also modulate the expression of CaSR, as we found that CAV1 overexpression restrained the COM-induced upregulation of CaSR.

Despite extensive studies on the mechanisms underlying kidney stone disease, the precise process of the stone formation remains incompletely understood, largely due to the absence of ideal experimental animal models. Hyperoxaluria is recognized as a crucial risk factor for development of kidney stones in humans. In the human body, oxalate is primarily excreted through glomerular filtration and renal tubular secretion[50]. Following urine concentration, oxalate levels reach the peak in the

collecting duct, which is a common initial site for CaOx crystal deposition. Research indicates that high concentrations of oxalate can induce morphological changes and damage to both proximal tubule and collecting duct cell lines, whereas lower concentrations do not produce such effects[51]. Injured cells exhibit an increased affinity for crystal attachment, promoting the retention of crystals within the renal collecting duct[52]. Therefore, hyperoxaluria-induced cellular damage is a critical factor in the formation of CaOx stones. Although rats are frequently used as model organisms for kidney stone disease research, their kidney structure differs from that of humans; for instance, rat kidneys are considerably smaller, possessing a single papillary and approximately 30,000 nephrons. Moreover, normal rats display substantially higher urinary oxalate concentrations compared to humans[53]. The mechanisms of kidney stone formation in humans are more intricate, influenced by various factors including genetics, diet, and environmental conditions. Consequently, these differences limit the applicability of our findings from rat models to human patients.

However, oxalate is processed similarly in both rat and human kidneys, involving glomerular filtration and tubular secretion[50]. Additionally, numerous similarities in the composition and pathogenesis in CaOx kidney stones between human and rats have been reported[53]. Specifically, CaOx stones in both species predominantly consist of calcium oxalate, organic matrix, and matrix proteins, with comparable ultrastructural characteristics. The initial site of crystal deposition is the collecting duct of the renal papilla, which ultimately leads to stone formation on the surface of the renal papilla. Moreover, experimentally induced renal crystal deposition in rats has also been consistently linked to cell damage. EG, a precursor for oxalate, when administered in drinking water, has been shown to effectively induce hyperoxaluria, crystalluria, and models of CaOx stone formation[54]. Therefore, our findings in rats provide a valuable reference for elucidating the mechanisms underlying CaOx stone formation. To further explore the relationship between our findings and human kidney stones, we extracted expression data for *CaSR*, *CAV1*, *EGFR*, and *AKT* from GSE73680, an expression profiling array from calcium stone patients in Japan. The results were consistent with

our experimental findings, further substantiating the significant role of the CaSR-CAV1-EGFR/AKT signaling axis in the formation of kidney stones.

5 Conclusion

In conclusion, we deeply explored the mechanism of ER stress in the process of kidney stone formation based on a multi-omics integration analysis, and for the first time, revealed the changes of CaSR-CAV1-EGFR/AKT signal axis during the formation of renal crystals. Our findings may provide a promising avenue for the prevention and treatment of kidney stones by targeting the CaSR-CAV1-EGFR/AKT signal axis.

Acknowledgments

We express our sincere gratitude to Rungroj, Urabe, Thorleifsson, and Oddsson *et al.* for providing the GWAS data, as well as to Taguchi *et al*. for the gene expression profile data of kidney stone patients (GSE73680), which serve as the foundation of our study.

Conflicts of Interest

All the authors declare that they have no conflicts of interest.

Funding

This study was supported by grants from the National Natural Science Foundation of China (82070722, 82300865 and 82470798), the Liaoning provincial Department of Education fund (LJKMZ20221788) and the Natural Science Foundation of Liaoning Province (2024-BS-276)

Author contributions

Xiuli Lu and Bing Gao conceived of the idea of this study. Yang Li, Baoyu Yang, Haozhen Wang and Ting Liu performed the experiments and analyzed the data. Yang Li and Baoyu Yang wrote the manuscript. Xiuli Lu and Bing Gao revised and prepared

the manuscript. All authors have reviewed and approved the paper.

Supplementary material

Supplementary Table 1. Mapping 261 candidate SNPs to 199 genes using SNP Annotation and Proxy Search.

Supplementary figure 1. CaSR-CAV1-EGFR/AKT signal axis was changed in kidney stone patients. The expression data of *CaSR* (a), *CAV1*(b), *EGFR* (c), *AKT1/AKT2/AKT3* (d-f) were extracted from GSE73680. The C group represents normal papillary tissue from patients without any kidney stones (n = 6). The N group represents normal papillary tissue from patients with calcium stones (n = 27). The P group represents the Randall's Plaque tissues from patients with calcium stones (n = 29). * $p < 0.05$; ** $p < 0.01$ vs. the C group.

Reference

[1] C. Pak, Kidney stones, Lancet (London, England), 351 (1998) 1797-1801.

[2] J. Asplin, Hyperoxaluric calcium nephrolithiasis, Endocrinology and metabolism clinics of North America, 31 (2002) 927-949.

[3] N. Rungroj, C. Nettuwakul, N. Sudtachat, O. Praditsap, N. Sawasdee, S. Sritippayawan, D. Chuawattana, P.T. Yenchitsomanus, A whole genome SNP genotyping by DNA microarray and candidate gene association study for kidney stone disease, BMC medical genetics, 15 (2014) 50.

[4] A. Oddsson, P. Sulem, H. Helgason, V.O. Edvardsson, G. Thorleifsson, G. Sveinbjörnsson, E. Haraldsdottir, G.I. Eyjolfsson, O. Sigurdardottir, I. Olafsson, G. Masson, H. Holm, D.F. Gudbjartsson, U. Thorsteinsdottir, O.S. Indridason, R. Palsson, K. Stefansson, Common and rare variants associated with kidney stones and biochemical traits, Nature communications, 6 (2015) 7975.

[5] G. Thorleifsson, H. Holm, V. Edvardsson, G.B. Walters, U. Styrkarsdottir, D.F. Gudbjartsson, P. Sulem, B.V. Halldorsson, F. de Vegt, F.C. d'Ancona, M. den Heijer, L. Franzson, C. Christiansen, P. Alexandersen, T. Rafnar, K. Kristjansson, G. Sigurdsson, L.A. Kiemeney, M. Bodvarsson, O.S. Indridason, R. Palsson, A. Kong, U. Thorsteinsdottir, K. Stefansson, Sequence variants in the CLDN14 gene associate with kidney stones and bone mineral density, Nature genetics, 41 (2009) 926-930.

[6] Y. Urabe, C. Tanikawa, A. Takahashi, Y. Okada, T. Morizono, T. Tsunoda, N. Kamatani, K. Kohri, K. Chayama, M. Kubo, Y. Nakamura, K. Matsuda, A genome-wide association study of nephrolithiasis in the Japanese population identifies novel susceptible Loci at 5q35.3, 7p14.3, and 13q14.1, PLoS genetics, 8 (2012) e1002541.

[7] B. Yang, X. Lu, Y. Li, Y. Li, D. Yu, W. Zhang, C. Duan, K. Taguchi, T. Yasui, K. Kohri, B. Gao, A Proteomic Network Approach across the Kidney Stone Disease Reveals Endoplasmic Reticulum Stress and Crystal-Cell Interaction in the Kidney, Oxidative medicine and cellular longevity, 2019 (2019) 9307256.

[8] S.J. Park, C. Li, Y.M. Chen, Endoplasmic Reticulum Calcium Homeostasis in Kidney Disease: Pathogenesis and Therapeutic Targets, The American journal of pathology, 191 (2021) 256-265.

[9] A.P. Arruda, G.S. Hotamisligil, Calcium Homeostasis and Organelle Function in the Pathogenesis of Obesity and Diabetes, Cell metabolism, 22 (2015) 381-397.

[10] R.S.G. Tan, C.H.L. Lee, H. Dimke, R. Todd Alexander, The role of calcium-sensing receptor

signaling in regulating transepithelial calcium transport, Experimental biology and medicine (Maywood, N.J.), 246 (2021) 2407-2419.

[11] G. Vezzoli, L. Macrina, G. Magni, T. Arcidiacono, Calcium-sensing receptor: evidence and hypothesis for its role in nephrolithiasis, Urolithiasis, 47 (2019) 23-33.

[12] S.S. Sundararaman, E.P.C. van der Vorst, Calcium-Sensing Receptor (CaSR), Its Impact on Inflammation and the Consequences on Cardiovascular Health, International journal of molecular sciences, 22 (2021).

[13] C. Liu, H. Li, H. Zheng, M. Zhai, F. Lu, S. Dong, T. Fang, W. Zhang, CaSR activates PKCδ to induce cardiomyocyte apoptosis via ER stress-associated apoptotic pathways during ischemia/reperfusion, International journal of molecular medicine, 44 (2019) 1117-1126.

[14] S.Y. Jung, J.O. Kwak, H.W. Kim, D.S. Kim, S.D. Ryu, C.B. Ko, S.H. Cha, Calcium sensing receptor forms complex with and is up-regulated by caveolin-1 in cultured human osteosarcoma (Saos-2) cells, Experimental & molecular medicine, 37 (2005) 91-100.

[15] Z.H. Wang, Q.H. Hu, H. Zhong, F.M. Deng, F. He, [Extracellular Ca(2+)-sensing receptor-induced extracellular Ca2+ influx is down-regulated by caveolin-1 in human umbilical vein endothelial cells], Sheng li xue bao : [Acta physiologica Sinica], 63 (2011) 39-47.

[16] T. Vanmierlo, V. Bloks, L. van Vark-van der Zee, K. Rutten, A. Kerksiek, S. Friedrichs, E. Sijbrands, H. Steinbusch, F. Kuipers, D. Lütjohann, M. Mulder, Alterations in brain cholesterol metabolism in the APPSLxPS1mut mouse, a model for Alzheimer's disease, Journal of Alzheimer's disease : JAD, 19 (2010) 117-127.

[17] S. Wang, N. Wang, Y. Zheng, J. Zhang, F. Zhang, Z. Wang, Caveolin-1: An Oxidative Stress-Related Target for Cancer Prevention, Oxid Med Cell Longev, 2017 (2017) 7454031.

[18] A. Barabási, N. Gulbahce, J. Loscalzo, Network medicine: a network-based approach to human disease, Nature reviews. Genetics, 12 (2011) 56-68.

[19] G. Zeng, Z. Mai, S. Xia, Z. Wang, K. Zhang, L. Wang, Y. Long, J. Ma, Y. Li, S. Wan, W. Wu, Y. Liu, Z. Cui, Z. Zhao, J. Qin, T. Zeng, Y. Liu, X. Duan, X. Mai, Z. Yang, Z. Kong, T. Zhang, C. Cai, Y. Shao, Z. Yue, S. Li, J. Ding, S. Tang, Z. Ye, Prevalence of kidney stones in China: an ultrasonography based cross-sectional study, BJU international, 120 (2017) 109-116.

[20] K. Lage, N. Hansen, E. Karlberg, A. Eklund, F. Roque, P. Donahoe, Z. Szallasi, T. Jensen, S. Brunak,

A large-scale analysis of tissue-specific pathology and gene expression of human disease genes and complexes, Proceedings of the National Academy of Sciences of the United States of America, 105 (2008) 20870-20875.

[21] A. Taylor, J. Steinberg, T. Andrews, C. Webber, GeneNet Toolbox for MATLAB: a flexible platform for the analysis of gene connectivity in biological networks, Bioinformatics (Oxford, England), 31 (2015) 442-444.

[22] P. Shannon, A. Markiel, O. Ozier, N. Baliga, J. Wang, D. Ramage, N. Amin, B. Schwikowski, T. Ideker, Cytoscape: a software environment for integrated models of biomolecular interaction networks, Genome research, 13 (2003) 2498-2504.

[23] d.W. Huang, B. Sherman, R. Lempicki, Systematic and integrative analysis of large gene lists using DAVID bioinformatics resources, Nature protocols, 4 (2009) 44-57.

[24] Y. Li, X. Lu, Z. Yu, H. Wang, B. Gao, Meta-data analysis of kidney stone disease highlights ATP1A1 involvement in renal crystal formation, Redox biology, 61 (2023) 102648.

[25] X. Lu, F. Kambe, X. Cao, T. Yoshida, S. Ohmori, K. Murakami, T. Kaji, T. Ishii, D. Zadworny, H. Seo, DHCR24-knockout embryonic fibroblasts are susceptible to serum withdrawal-induced apoptosis because of dysfunction of caveolae and insulin-Akt-Bad signaling, Endocrinology, 147 (2006) 3123-3132.

[26] G. Di Conza, P.C. Ho, ER Stress Responses: An Emerging Modulator for Innate Immunity, Cells, 9 (2020).

[27] J. Moreno-Càceres, D. Caballero-Díaz, Z.C. Nwosu, C. Meyer, J. López-Luque, A. Malfettone, R. Lastra, T. Serrano, E. Ramos, S. Dooley, I. Fabregat, The level of caveolin-1 expression determines response to TGF-β as a tumour suppressor in hepatocellular carcinoma cells, Cell death & disease, 8 (2017) e3098.

[28] J. Qu, T. Zou, Z. Lin, The Roles of the Ubiquitin-Proteasome System in the Endoplasmic Reticulum Stress Pathway, International journal of molecular sciences, 22 (2021).

[29] E. Codrici, L. Albulescu, I. Popescu, S. Mihai, A. Enciu, R. Albulescu, C. Tanase, M. Hinescu, Caveolin-1-Knockout Mouse as a Model of Inflammatory Diseases, Journal of immunology research, 2018 (2018) 2498576.

[30] C.J. Liu, C.W. Cheng, Y.S. Tsai, H.S. Huang, Crosstalk between Renal and Vascular Calcium

Signaling: The Link between Nephrolithiasis and Vascular Calcification, International journal of molecular sciences, 22 (2021).

[31] G. Vezzoli, A. Terranegra, F. Rainone, T. Arcidiacono, M. Cozzolino, A. Aloia, E. Dogliotti, D. Cusi, L. Soldati, Calcium-sensing receptor and calcium kidney stones, Journal of translational medicine, 9 (2011) 201.

[32] A. Balistrieri, A. Makino, J.X. Yuan, Pathophysiology and pathogenic mechanisms of pulmonary hypertension: role of membrane receptors, ion channels, and Ca(2+) signaling, Physiological reviews, 103 (2023) 1827-1897.

[33] F.C. Gombedza, S. Shin, Y.L. Kanaras, B.C. Bandyopadhyay, Abrogation of store-operated Ca(2+) entry protects against crystal-induced ER stress in human proximal tubular cells, Cell death discovery, 5 (2019) 124.

[34] H.L. Ong, X. Liu, K. Tsaneva-Atanasova, B.B. Singh, B.C. Bandyopadhyay, W.D. Swaim, J.T. Russell, R.S. Hegde, A. Sherman, I.S. Ambudkar, Relocalization of STIM1 for activation of store-operated Ca(2+) entry is determined by the depletion of subplasma membrane endoplasmic reticulum Ca(2+) store, The Journal of biological chemistry, 282 (2007) 12176-12185.

[35] X. Li, J. Ma, W. Shi, Y. Su, X. Fu, Y. Yang, J. Lu, Z. Yue, Calcium Oxalate Induces Renal Injury through Calcium-Sensing Receptor, Oxidative medicine and cellular longevity, 2016 (2016) 5203801.

[36] V. Tam, N. Patel, M. Turcotte, Y. Bossé, G. Paré, D. Meyre, Benefits and limitations of genome-wide association studies, Nature reviews. Genetics, 20 (2019) 467-484.

[37] Y. Lai, H. Zheng, X. Sun, J. Lin, Q. Li, H. Huang, Y. Hou, H. Zhong, D. Zhang, T. Fucai, Z. He, The advances of calcium oxalate calculi associated drugs and targets, European journal of pharmacology, 935 (2022) 175324.

[38] G. Cao, G. Yang, T.L. Timme, T. Saika, L.D. Truong, T. Satoh, A. Goltsov, S.H. Park, T. Men, N. Kusaka, W. Tian, C. Ren, H. Wang, D. Kadmon, W.W. Cai, A.C. Chinault, T.B. Boone, A. Bradley, T.C. Thompson, Disruption of the caveolin-1 gene impairs renal calcium reabsorption and leads to hypercalciuria and urolithiasis, The American journal of pathology, 162 (2003) 1241-1248.

[39] L. Xu, X. Qu, H. Li, C. Li, J. Liu, H. Zheng, Y. Liu, Src/caveolin-1-regulated EGFR activation antagonizes TRAIL-induced apoptosis in gastric cancer cells, Oncology reports, 32 (2014) 318-324.

[40] J. Brüning, D. Gautam, D. Burks, J. Gillette, M. Schubert, P. Orban, R. Klein, W. Krone, D. Müller-

Wieland, C. Kahn, Role of brain insulin receptor in control of body weight and reproduction, Science (New York, N.Y.), 289 (2000) 2122-2125.

[41] J. Park, H. Han, Caveolin-1 plays important role in EGF-induced migration and proliferation of mouse embryonic stem cells: involvement of PI3K/Akt and ERK, American journal of physiology. Cell physiology, 297 (2009) C935-944.

[42] J. Moreno-Càceres, D. Caballero-Díaz, Z. Nwosu, C. Meyer, J. López-Luque, A. Malfettone, R. Lastra, T. Serrano, E. Ramos, S. Dooley, I. Fabregat, The level of caveolin-1 expression determines response to TGF-β as a tumour suppressor in hepatocellular carcinoma cells, Cell death & disease, 8 (2017) e3098.

[43] Y. Yang, S. Hong, Y. Lu, Q. Wang, S. Wang, Y. Xun, CAV1 alleviated CaOx stones formation via suppressing autophagy-dependent ferroptosis, PeerJ, 10 (2022) e14033.

[44] Y. Shu, S. Jin, Caveolin-1 in endothelial cells: A potential therapeutic target for atherosclerosis, Heliyon, 9 (2023) e18653.

[45] C.Y. Lee, T.Y. Lai, M.K. Tsai, Y.C. Chang, Y.H. Ho, I.S. Yu, T.W. Yeh, C.C. Chou, Y.S. Lin, T. Lawrence, L.C. Hsu, The ubiquitin ligase ZNRF1 promotes caveolin-1 ubiquitination and degradation to modulate inflammation, Nature communications, 8 (2017) 15502.

[46] A. Hayer, M. Stoeber, D. Ritz, S. Engel, H.H. Meyer, A. Helenius, Caveolin-1 is ubiquitinated and targeted to intralumenal vesicles in endolysosomes for degradation, The Journal of cell biology, 191 (2010) 615-629.

[47] V. Sathish, A.J. Abcejo, S.K. VanOosten, M.A. Thompson, Y.S. Prakash, C.M. Pabelick, Caveolin-1 in cytokine-induced enhancement of intracellular Ca(2+) in human airway smooth muscle, American journal of physiology. Lung cellular and molecular physiology, 301 (2011) L607-614.

[48] O. Kifor, I. Kifor, F.D. Moore, Jr., R.R. Butters, Jr., T. Cantor, P. Gao, E.M. Brown, Decreased expression of caveolin-1 and altered regulation of mitogen-activated protein kinase in cultured bovine parathyroid cells and human parathyroid adenomas, The Journal of clinical endocrinology and metabolism, 88 (2003) 4455-4464.

[49] R.K. Batori, F. Chen, Z. Bordan, S. Haigh, Y. Su, A.D. Verin, S.A. Barman, D.W. Stepp, T. Chakraborty, R. Lucas, D.J.R. Fulton, Protective role of Cav-1 in pneumolysin-induced endothelial barrier dysfunction, Frontiers in immunology, 13 (2022) 945656.

[50] S. Robijn, B. Hoppe, B.A. Vervaet, P.C. D'Haese, A. Verhulst, Hyperoxaluria: a gut-kidney axis?, Kidney international, 80 (2011) 1146-1158.

[51] M.S. Schepers, E.S. van Ballegooijen, C.H. Bangma, C.F. Verkoelen, Oxalate is toxic to renal tubular cells only at supraphysiologic concentrations, Kidney international, 68 (2005) 1660-1669.

[52] J.H. Wiessner, A.T. Hasegawa, L.Y. Hung, G.S. Mandel, N.S. Mandel, Mechanisms of calcium oxalate crystal attachment to injured renal collecting duct cells, Kidney international, 59 (2001) 637-644.

[53] S.R. Khan, Animal models of calcium oxalate kidney stone formation，in: Animal Models for the Study of Human Disease, Elsevier, (2013) 483-498.

[54] D.T. Tzou, K. Taguchi, T. Chi, M.L. Stoller, Animal models of urinary stone disease, International journal of surgery (London, England), 36 (2016) 596-606.

Figures Legends

Figure 1. CaSR-mediated intracellular Ca^{2+} overload participated in the COM-induced ER stress in HK-2 cells. After pretreatment with 10 μM NPS2390 for 1 hour, HK-2 cells were exposed to 100 μg/mL COM for 6 hours. The intracellular Ca^{2+} level was detected with Fluo-4 AM (a) and was expressed as the relative fluorescence intensity, calculated as fold changes relative to the COM(－) group (b). The expression of CaSR, Bip, CHOP, ATF6, XBP-1 and the phosphorylated PERK were detected by western blotting (c). The relative expression levels of these proteins were expressed as a fold change relative to the level in the COM(－) group (d-i). All experiments were repeated at least thrice, independently. *$p < 0.05$, **$p < 0.01$, ****$p < 0.0001$ vs. COM(－); #$p < 0.05$, ##$p < 0.01$, ###$p < 0.001$ vs. only COM(＋).

Figure 2. The network analysis of GWAS data and microarray data in patients with kidney stones. A workflow corresponding to network analysis of GWAS and microarray datasets is shown (a). The PPI network containing 38 highly connected nodes was constructed (b). The KEGG pathway of the GWAS data was analyzed (c). The PPI network of the microarray data contained 345 highly connected nodes. Red nodes are the top 10% hub genes, ranked based on Node degree, BC, and Edge Betweenness (d). The KEGG enrichment analysis of the microarray data was conducted (e). The overlap between GWAS network nodes and microarray network nodes included six genes: *DMBT1*, *ZNF408*, *CAV1*, *LRP2*, *CAV2*, and *HSPG2* (f). The overlap between GWAS KEGG pathways and microarray KEGG pathways contained two pathways: focal adhesion and proteoglycans in cancer (g). The focal adhesion pathway with three transmembrane receptors (ECM-receptor, CAV, and RTK) plays an important role in cell proliferation, regulation of gene expression, and cell survival. SNP rs6867 was genotyped using HRM. Each sample was repeated at least three times independently. The results were determined by the difference plots (h) and the aligned melt curves (i). Two genotypes were identified. The green curves represent the wild type (GG) and the blue curves represent the heterozygote type (GA). Sanger sequencing

revealed complete consistency with the HRM results. The black arrows indicate SNP rs6867 (j).

Figure 3. COM-induced the post-translational degradation of CAV1 damage to EGFR/AKT cell survival signaling pathway. After exposing HK-2 cells to 100 μg/mL COM for 24 or 48 hours, apoptosis was detected using TUNEL assays (a). The percentage of TUNEL positive cells was expressed as the ratio of apoptotic cells to adherent cells (b). $^{**}p < 0.01$, $^{***}p < 0.001$ vs. 0h. CAV1 was observed using immunocytochemistry in HK-2 cells after being exposed to CaOx crystals for 48 hours. Red fluorescence represents CAV1 expression and blue fluorescence represents DAPI-stained nuclei (c). The relative fluorescence intensity was calculated as the fold change relative to the control group (d). $^{**}p < 0.01$ vs. the control group. The protein expression of CAV1 and the phosphorylation levels of EGFR and AKT were determined using western blotting (e-h). $^{*}p < 0.05$, $^{**}p < 0.01$ vs. the level at 0h. The mRNA expression of *CAV1* was measured using qRT–PCR (i). n = 3. To investigate whether COM-induced CAV1 decline was related to the post-translational degradation, HK-2 cells were pretreated with 20μM MG132 and then exposed to COM for 48 hours to detect the CAV1 expression with western blotting (j). $^{**}p < 0.01$ vs. the group without COM(－) and MG132(－); $\#\#p < 0.01$ vs. the group only with COM(+). All experiments were repeated at least thrice, independently.

Figure 4. CAV1 overexpression protected HK-2 cells from apoptosis induced by COM. 48 hours after infection with HBAD-hCAV1, the protein level of CAV1 in HK-2 cells was detected by western blotting (a and b). $^{***}p < 0.001$ vs. HBAD-Null. The effect of CAV1 overexpression on COM-induced apoptosis was explored using TUNEL assays (c). The percentage of TUNEL-positive cells was expressed as the ratio of apoptotic cells to the adherent cells (d). $^{**}p < 0.01$, $^{****}p < 0.0001$ vs.COM(－); $\#\#\#\#p < 0.0001$ vs. COM(+) in HBAD-Null. The level of cleaved-caspase 3 was measured using western blotting (e-f). $^{***}p < 0.001$ vs. HBAD-Null. Crystal-cell

adhesion was measured using atomic absorption to determine calcium concentration (g). *$p < 0.05$ vs. HBAD-Null. ###$p < 0.001$ vs. the control group. The phosphorylation Fluo-4 AM levels of EGFR and AKT were also detected using western blotting (h-j). **$p < 0.01$, ***p <0.001vs. HBAD-Null. The relative levels of all proteins were expressed as fold changes relative to the levels at 0 hour in each group. All experiments were repeated at least thrice, independently.

Figure 5. CAV1 overexpression inhibited COM-induced ER stress. The effect of CAV1 on the intracellular Ca^{2+} level was detected uisng Fluo-4 AM (a and b). *$p < 0.05$, ***$p < 0.001$ vs.COM(－); ##$p < 0.01$ vs. COM(+) in HBAD-Null. The effects of CAV1 overexpression on COM-induced ER stress were determined by measuring the expressions of Bip, CHOP, ATF6, XBP-1, phosphorylated PERK and CASR with western blotting (c). The relative levels of all proteins were expressed as fold changes relative to the levels at 0 hour in each group (d-i). **$p < 0.01$, ***$p < 0.001$, ****$p <$ 0.0001 vs. HBAD-Null. All the experiments were repeated at least thrice, independently.

Figure 6. Changes of CaSR-CAV1-EGFR/AKT signaling axis in rats treated with 0.75% EG for 8 weeks. The CaOx stone rat model was induced by giving 0.75% EG in the drinking water (n = 5 in each group). Crystals were formed from week 2. The red arrow indicates the crystal. Scale bar = 100 μM (a). Small inflammatory foci were found in renal tissues of rats at week 8 (yellow arrow). Severe congestion and dilation of capillaries were observed at the junction of medulla and cortex (black arrow). The blue arrow represents mild congestion. Scale bar = 100 μM (b). The CAV1 levels in the rat kidneys were tested by immunohistochemical staining. Scale bar = 25 μM. Relative mean optical density (MOD) was calculated as fold changes relative to the value in the control group (d-f). ***$p < 0.001$, ****$p < 0.0001$ vs. the control group. Western blotting was used to detect the expression of CAV1 in the rat renal tissues (g). The relative expression of the protein was calculated as fold changes relative to the level in the control group (h). **$p < 0.01$, **** $p < 0.0001$ vs. the control group. CAV1 mRNA

expression was determined using qRT–PCR and was shown unchanged (i).

Figure 7: The CaSR expression and the EGFR/AKT signaling pathway in renal crystal rats were changed. The levels of CaSR and the phosphorylated EGFR and AKT were measured with western blotting (a). The relative expressions of these proteins were calculated as fold changes relative to the level in the control group (b-d). *$p < 0.05$, **$p < 0.01$, *** $p < 0.001$, **** $p < 0.0001$ vs. the control group. Each experiment was repeated at least thrice, independently.

Figure 8: Schematic diagram of the mechanism of CaSR-CAV1-EGFR/AKT signal axis during the formation of renal crystals. ① COM increased the intracellular Ca^{2+} level by up-regulating CaSR expression. ② Overload of the intracellular Ca^{2+} level led to ER stress. ③-④ Sustained ER stress activated post-translational degradation of CAV1. ⑤-⑥ The degradation of CAV1 impaired the EGFR-AKT cell survival signaling pathway and exacerbated ER stress by affecting CaSR function, ultimately causing HK-2 apoptosis. ⑦ The damaged HK-2 cells further promoted the adhesion of crystals to the cell surface.

Table 1. SNPs in the four hub genes from the GWAS PPI network

SNPs	Chromosome	Position	Alleles	Genes
rs7801956	7	55181937	A/G	*EGFR*
rs5031002	X	66859350	A/G	*AR*
rs6867	7	115987759	A/G	*CAV1*
rs12444784	16	67359924	A/G	*CDH1*

Table 2. The statistics of genotype and allele frequencies of SNP rs6867 (G>A) in patients with kidney stones

Gene	SNP rs6867	No. cases (%)	No. controls (%)	OR (95%CI)	Chi-square	*p* value
CAV1	Genotype					
	GG	306 (96.23)	1148 (98.12)	2.046(1.001 - 4.181)	4.014	0.0451*
	GA	12 (3.77)	22 (1.88)	—	—	—
	Allele					
	G	624(98.11)	2318(99.06)	2.026(0.997 - 4.117)	3.968	0.0464*
	A	12(1.89)	22(0.94)	—	—	—

*$p < 0.05$

Controls are from the East Asian population in the 1000 Genomes Project database

Highlights

- Calcium oxalate induces endoplasmic reticulum stress by CaSR-mediated Ca^{2+} influx
- Caveolin-1 was decreased in rat models and patients with kidney stones
- Caveolin-1 affects the EGFR/AKT cell survival signaling pathway
- Caveolin-1 regulates CaSR-mediated Ca^{2+} influx induced by calcium oxalate